

Laboratori Nazionali di Frascati

LNF-69/57

C. Castagnoli, G. Silvestro, P. Picchi and G. Verri : ON THE POLARIZATION OF COHERENT RADIO SIGNALS FROM EAS.

Estratto da : Nuovo Cimento 63B, 373 (1969).

C. CASTAGNOLI, *et al.*
11 Settembre 1969
Il Nuovo Cimento
Serie X, Vol. 63 B, pag. 373-384

On the Polarization of Coherent Radio Signals from EAS.

C. CASTAGNOLI and G. SILVESTRO

Laboratorio di Cosmo-geofisica del CNR
Istituto di Fisica Generale dell'Università - Torino

P. PICCHI and G. VERRI

Laboratori Nazionali del CNEN - Frascati

(ricevuto il 9 Aprile 1969)

Summary. — The influence of the geomagnetic field on EAS radio emission is analysed by simulating with a three-dimensional Monte Carlo the development of an e.m. cascade in the earth's magnetic field taking full account of Coulomb scattering. We compute for vertical showers at various heights the dipole moment M , the transverse current J , together with the negative charge excess ϵ . A discussion of the radiation field shows that the geomagnetic effect is appreciably less than previously estimated and depends on frequency. The polarization of the observed signal decreases markedly with increasing frequency, which seems to agree with experimental data.

1. — Introduction.

The polarization of coherent radio signals associated with extensive air showers (EAS) is an open problem both on observational and theoretical grounds.

Various mechanisms have been suggested for the origin of the coherent emission observed (¹⁻¹⁰) from EAS. According to ASKARYAN (^{11,12}) it should

(¹) J. V. JELLEY, J. H. FRUIN, N. A. PORTER, T. C. WEEKES, F. G. SMITH and R. A. PORTER: *Nature*, **205**, 327 (1965).

(²) N. A. PORTER, C. D. LONG, B. McBRENN, D. J. B. MURNAGHAN and T. C. WEEKES: *Phys. Rev. Lett.*, **19**, 415 (1965).

(³) J. V. JELLEY, N. CHARMAN, J. H. FRUIN, S. GRAHAM SMITH, N. A. PORTER, R. A. PORTER, B. McBRENN and J. C. WEEKES: *Nuovo Cimento*, **46 A**, 649 (1966).

(⁴) I. A. BORSKOVSKY, V. D. VOLOVIK, V. I. KOBIZSKOY and E. S. SHMATKO: *Sov. Phys. JETP Lett.*, **3**, 118 (1966).

(⁵) H. R. ALLAN, J. K. JONES, K. P. NEAT and R. W. CLAY: in *Bi-Annual News-*

come from an electron excess in the shower front, the enhancement factor with respect to incoherent radiation being $I_{coh}/I_{incoh} \approx \varepsilon^2 N$, where $\varepsilon = 2(N^- - N^+)/N$ is the fractionary charge excess, N^- , N^+ , N are the number of electrons and positrons and the total number of particles in the EAS. The radiation from the charge excess is radially polarized as the ordinary Čerenkov radiation.

According to KAHN and LERCHE (18), instead, the EAS radio emission is mainly due to the charge separation in the earth's magnetic field, which induces a polarization and a transverse current in the shower front. They estimate a signal from the geomagnetic effect about one order of magnitude larger than from the excess charge, the radiation being almost completely polarized in the E-W direction, and the energy received on the ground per unit area per unit band width $I(\nu) \sim \nu^2$.

Our purpose is to investigate the polarization, by evaluating at various heights the quantities relevant to the radio emission (the negative excess ε , the dipole moment M , the transverse current J), and taking into consideration not only the geomagnetic deflection but also Coulomb scattering, which was disregarded previously. An analytic treatment of the EAS development in the geomagnetic field, though limited to the electromagnetic cascade, would be a heavy task, and we shall use an accurate Monte Carlo technique. Our results (Sect. 2) give a charge excess lower than estimated by ASKARYAN, and a substantial decrease in the geomagnetic effect with respect to the Kahn and Lerche estimate. A discussion of the radiation field (Sect. 3) yields the frequency dependence of the signal from the two mechanisms, from which we estimate the polarization to be expected at the various frequencies, which is shown to be in agreement with experimental data (Sect. 4).

2. — Calculation, results and discussion of EAS parameters.

Our calculation is a tridimensional Monte Carlo (the magnetic field suppresses the axial symmetry of the cascade) in approximation B . The cascade devel-

letters of British Universities, EAS Project at Haverah Park, November, 1968.

(⁶) S. N. VERNOV, A. T. ABROSIMOV, V. D. VOLOVIK, I. I. ZABYUBOVSKII and G. B. KRISTIANSEN: *Sov. Phys. JETP Lett.*, **5**, 126 (1967).

(⁷) P. R. BARKER, W. E. HAZEN and A. Z. HENDEL: *Can. Journ. Phys.*, **46**, 243 (1968).

(⁸) R. A. PORTER, F. G. SMITH and W. S. TORBITT: *Nature*, **213**, 1107 (1967).

(⁹) J. R. PRESCOTT, G. C. PALUMBO, C. H. COSTAIN and J. A. GALT: *Can. Journ. Phys.*, **46**, 246 (1968).

(¹⁰) W. E. HAZEN, A. Z. HENDEL, H. SMITH and N. J. SHAH: *Phys. Rev. Lett.*, **22**, 35 (1969).

(¹¹) G. A. ASKARYAN: *Sov. Phys. JETP*, **14**, 441 (1962).

(¹²) G. A. ASKARYAN: *Sov. Phys. JETP*, **21**, 658 (1965).

(¹³) F. D. KAHN and I. LERCHE: *Proc. Roy. Soc., A* **289**, 206 (1966).

ops along the z -axis, the magnetic deviation is in the x -direction. The computer follows each particle, taking into account the cascade processes (bremsstrahlung, pair production, multiple scattering and ionization energy loss) together with e^+ annihilation, and evaluates the magnetic displacement for each particle in the path between two radiation processes.

The well-known formulae⁽¹⁴⁾ are used for the collision energy loss of electrons with energy $E \gg mc^2$. Radiation and pair production processes are treated with the complete screening cross-sections of BETHE and HEITLER⁽¹⁵⁾, assuming a minimum value $v = 10^{-3}$ for the photon fractionary energy in radiation processes, below which limit radiation loss is considered continuous. The angular distribution of the particles from these processes is given by Bethe's approximate formulae⁽¹⁶⁾. The usual Molière's relation⁽¹⁷⁾ is assumed for the distribution of the scattering angle Φ in multiple-scattering processes.

The particles are assigned an index I according to the order of production, and an index $T = +1, -1$ is given to e^+ and e^- , respectively. The particle with the highest I is followed, memorizing all quantities relative to secondary branches: whenever this particle reaches one of the three reference heights, the computer memorizes its energy E , the position x, y , the polar angles θ, φ of the velocity (the particle is discarded when its energy falls below the Čerenkov threshold $E_c(h)$). Then the procedure starts over again with the $(I-1)$ -th particle. The calculation is concluded when all branches have been followed ($I=0$).

Vertical showers are simulated, originated by γ -rays with energy $E_\gamma = 10^{12}, 10^{13}, 10^{14}$ eV, at the height $h = 15$ km above sea level (the zenith angle distribution of EAS can be written⁽¹⁸⁾ as $\mathcal{I}(\theta) \sim \cos^n \theta$, with $n \sim 6$ at sea level, therefore a large majority of the radio showers striking the apparatus are about vertical). The horizontal component of the geomagnetic field is⁽¹⁹⁾ $B = 0.31 \cos \lambda$ G, where λ is the geomagnetic latitude: we assume in our calculation $B_\perp = 0.3$ G. Appendix I gives the formulae for magnetic deviation and e^+ annihilation.

For each energy we obtain, at $h = 5, 6, 8$ km, the total number N of particles with energy above the Čerenkov threshold $E_c(h)$, the number N^-, N^+ of electrons and positrons, the fractionary charge excess ε , the mean separation Δ of electrons and positrons in the E-W direction, the dipole moment $M = e \left(\sum_{e^+} x^+ - \sum_{e^-} x^- \right) = eN\Delta$, the total current $J_x = e \left(\sum_{e^+} v_x^+ - \sum_{e^-} v_x^- \right)$ and J_y in

⁽¹⁴⁾ B. ROSSI: *High-Energy Particles*, Chap. 2 (Englewood Cliffs., N. J., 1952).

⁽¹⁵⁾ H. BETHE and W. HEITLER: *Proc. Roy. Soc.*, **83**, 146 (1934).

⁽¹⁶⁾ H. BETHE: *Proc. Camb. Phil. Soc.*, 524 (1934).

⁽¹⁷⁾ C. MOLIÈRE: *Zeits. Naturforsch.*, **3 A**, 78 (1948).

⁽¹⁸⁾ W. GALBRAITH: *Extensive Air Showers*, Chap. 5 (London, 1958).

⁽¹⁹⁾ G. COCCONI: *Phys. Rev.*, **93**, 646 (1954).

the E-W and N-S directions, the mean transverse velocities v_x and v_y . These quantities are computed also in a series of rings about the axis of the shower.

The results have been favourably checked by comparing with the theoretical curves for the electromagnetic cascade given by SNYDER⁽²⁰⁾, and the lateral distribution of GREISEN⁽²¹⁾ and NISHIMURA-KAMATA⁽²²⁾. Figure 1 shows our

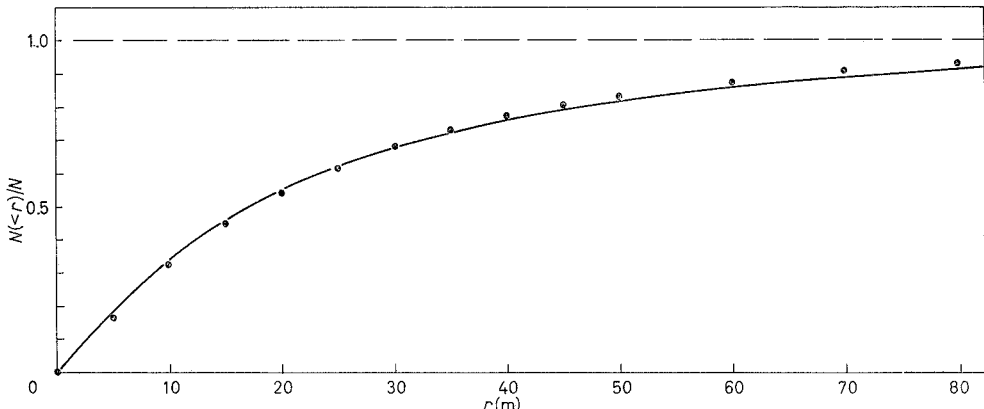


Fig. 1. – Lateral distribution of the particles in the e.m. cascade. The solid curve gives the fraction of particles within the distances r from the axis according to Greisen's lateral distribution function (formula (1), with $r_1 = 29.4$ m). The points are our Monte Carlo results at $E_\gamma = 10^{13}$ eV, $h = 5$ km.

Monte Carlo results at $E_\gamma = 10^{13}$ eV, $h = 5$ km, for the fraction of particles within a distance r from the axis, together with the theoretical curves given by the authors. One can see that our results are beautifully fitted by the lateral distribution given by GREISEN,

$$(1) \quad n(r) dr = 2\pi r \frac{0.4N}{r_1^2} \left(\frac{r}{r_1}\right)^{-0.75} \left(\frac{r}{r_1} + 1\right)^{-3.25} \left(1 + \frac{r/r_1}{11.4}\right) dr,$$

when one assumes $r_1 = 29.4$ m (our distribution refers to particles with $E > E_c$).

Table I gives at the three heights considered the values of ε , Δ , \bar{v}_x for the different shower energies.

The excess negative charge in EAS results from e^+ annihilation, and the addition to the cascade of electrons from knock-on and Compton processes: $\varepsilon = \varepsilon_{an} + \varepsilon_{ko} + \varepsilon_{co}$. ASKARYAN⁽¹¹⁾ assumed $\varepsilon = \varepsilon_{an}$ and evaluated $\varepsilon \simeq 0.1$; he performed the calculation at the positron mean energy $\langle E^+ \rangle = 100$ MeV, by

(20) H. S. SNYDER: *Phys. Rev.*, **76**, 1563 (1949).

(21) K. GREISEN: *Ann. Rev. Nucl. Sci.*, **10**, 63 (1960).

(22) J. NISHIMURA and K. KAMATA: *Progr. Theor. Phys.*, **7**, 185 (1952).

TABLE I.

h (km)	$E_\gamma = 10^{12}$ eV			$E_\gamma = 10^{13}$ eV			$E_\gamma = 10^{14}$ eV		
	ε	A (m)	\bar{v}_x (m/s)	ε	A (m)	\bar{v}_x (m/s)	ε	A (m)	\bar{v}_x (m/s)
5	0.046	1.19	$1.26 \cdot 10^6$	0.024	4.39	$2.42 \cdot 10^6$	0.010	4.14	$2.26 \cdot 10^6$
6	0.022	2.09	$1.68 \cdot 10^6$	0.035	4.49	$2.13 \cdot 10^6$	0.017	4.37	$2.16 \cdot 10^6$
8	0.013	2.34	$1.28 \cdot 10^6$	0.015	5.32	$2.08 \cdot 10^6$	0.049	4.95	$2.25 \cdot 10^6$

comparing the annihilation lifetime τ_{an} with the radiation lifetime $\tau_{\text{rad}} \sim I_{\text{rad}}/c$. But the lower-energy particles, which should give the main contribution to the charge excess ($\sigma_{\text{an}} \sim 1/E$), lose energy very fast in collision processes, and have no time to annihilate before going under the Čerenkov threshold.

We calculated ε_{an} with our Monte Carlo and assumed $\varepsilon_{\text{ko}} + \varepsilon_{\text{co}} = 2\varepsilon_{\text{an}}$ according to the results of GUZHAVIN *et al.* (23). Our results averaged over E_γ and h (Table I shows that ε_{an} is substantially independent, apart from fluctuations, of these quantities) give $\varepsilon_{\text{an}} = 2.5 \cdot 10^{-2}$, in agreement with Guzhavin's calculation. We obtain thus finally for the total charge excess $\varepsilon = (7 \pm 1) \cdot 10^{-2}$.

Figure 2 shows our Monte Carlo results for the net charge within the distance r , normalized to the total number of particles N and averaged over E_γ and h , from which we can obtain an empirical formula for the radial dependence

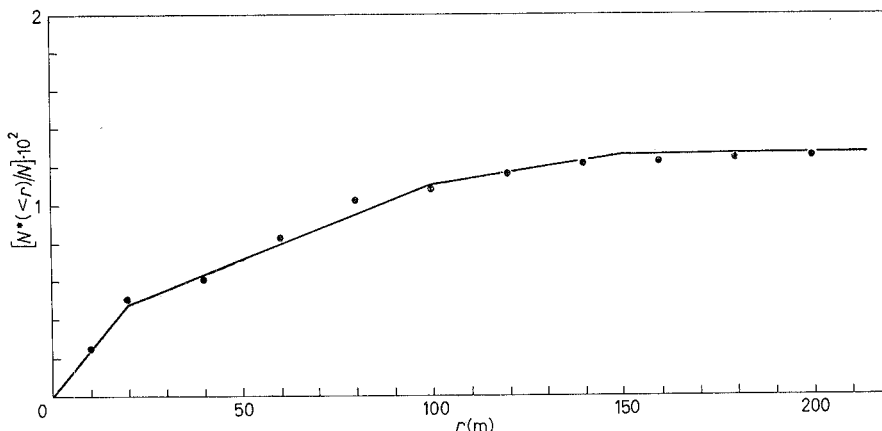


Fig. 2. – The net charge $N^*(< r)/N = (N^-(< r) - N^+(< r))/N$ within the distance r from the axis. The points are our Monte Carlo results averaged over E and h , the solid line is from the empirical function (2) (see text).

(23) V. V. GUZHAVIN, I. P. IVANENKO and A. E. LEVITIN: *Can. Journ. Phys.*, **46**, 209 (1968).

of the excess charge,

$$(2) \quad n^*(r) = \frac{1}{2} \epsilon(r) n(r) = a \cdot 10^{-4} N ,$$

with $a = 7.5, 2.25, 0.60, 0$ when $r(m) = 0 \div 20, 20 \div 100, 100 \div 150, > 150$.

Due to the difficulty of our Monte Carlo (each shower particle is followed in the program) we could not go beyond $E_\gamma = 10^{14}$ eV. In the range of energies considered, the mean displacement and mean velocity v_x are reasonably independent of E_γ . The pionization+isobar model for nucleon-nucleon interactions at high energy (24) gives a maximum energy E_γ in the laboratory frame for the γ -rays from the isobar's neutral pions which is about 3 % of the energy E_0 of the incident nucleon. The energy range $E_\gamma = (10^{12} \div 10^{14})$ eV for our electromagnetic cascades corresponds thus to EAS energies up to $E_0 \sim 10^{16}$ eV.

The influence of the geomagnetic field should depend essentially on the energetic and lateral distribution of the shower particles, and it is well known (see for instance (21)) that the energy spectrum of the EAS particles has been found to be remarkably independent of the size of the shower and the elevation, while the lateral distribution of the electromagnetic component (which alone contributes to the radio emission) is well represented by relation (1) (with a suitable value of r_1) for showers of size ranging from $2 \cdot 10^3$ to $2 \cdot 10^9$ charged particles, at elevations from sea level to 5200 m, and distances from the shower axis running up to 1500 m. We conclude our Monte Carlo results can be reasonably applied to typical radio showers, with energy $(10^{15} \div 10^{17})$ eV.

One sees Δ increases with height, due to the reduced importance of Coulomb scattering and the longer mean free path of particle interactions. The dependence of \bar{v}_x on h is very weak: indeed $\bar{v}_x \sim \tau/E$, where $\tau \sim \exp[h]$ is the mean time interval between two interactions, and the increase in τ goes together with an increase in E , while Δ depends quadratically on τ , $\Delta \sim \tau^2/E$.

Figure 3 shows the strong dependence of \bar{v}_x (averaged over E_γ and h) on the distance r from the axis (the uncertainty is assumed to be $\pm \bar{v}_x$, contributed by Coulomb scattering): \bar{v}_x goes to zero at $r = 0$, and increases about linearly with r till $r \sim 100$ m. The lateral velocity distribution from our results can be represented with the empirical function

$$(3) \quad v_x(r) = \begin{cases} 10^5 r \text{ (m/s)} & \text{when } r \leq 100 \text{ m ,} \\ 10^7 \text{ (m/s)} & \text{when } r > 100 \text{ m .} \end{cases}$$

The average over E_γ , h and r is $\bar{v}_x = (2.01 \cdot 10^6)$ m/s, while at $B_\perp = 0.3$ G the Kahn and Lerche value is $(v_x)_{KL} = 8 \cdot 10^6$ m/s. The mean separation is reduced by almost the same factor, being $\Delta_{KL} = 14.2$ m.

(24) Y. PAL and B. PETERS: *Mat. Fys. Medd.*, **33**, n. 15 (1964).

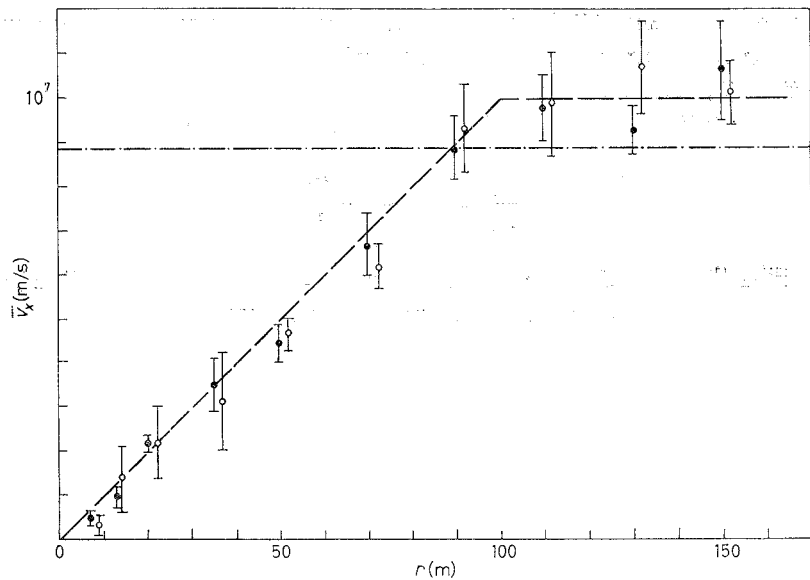


Fig. 3. — The mean transverse velocity \bar{v}_x in the E-W direction at $h = 5$ km. The uncertainty reported is $\pm \bar{v}_y$, the mean transverse velocity in the N-S direction. The dashed line is the empirical analytic approximation (3), the dash-dot line is the Kahn and Lerche value at $B = 0.3$ G. • $E_\gamma = 10^{13}$ eV; ○ $E_\gamma = 10^{14}$ eV.

3. — The radiation field.

A simplified evaluation of the radiation field can be given at distances R from the axis greater than the radius of the disc of charges (such that $n(R) \approx 0$), by phase mixing the contribution from the various rings. We compare first the current and space charge fields.

The Fourier components, with wave number $k = 2\pi r/c$ of the electric fields from the space charge E_s and current E_c at a distance R from the axis are found by integrating over the disc the relations given by KAHN and LERCHE for the radiation from one ring:

$$(4) \quad E_s(R) = -\frac{1}{4} ik\alpha e H_0^{(1)}(k\alpha R) \int_0^R J_0(k\alpha r) n(r) \epsilon(r) dr ,$$

$$(5) \quad E_c(R) = -\frac{ke}{2e} H_0^{(1)}(k\alpha R) \int_0^R J_0(k\alpha r) n(r) v(r) dr ,$$

where (J_0) and $H_0^{(1)}$ are the Bessel function of the first kind and the Hankel function.

Equations (4) and (5) have been integrated numerically at various frequencies for $h = 5$ km, with the lateral distribution $n(r)$ given by (1), the charge distribution (2) and the velocity distribution (3). Figure 4 shows the results of our computations. When full coherence holds, we have

$$\left| \frac{E_c}{E_s} \right| = 2 \frac{v}{c} \frac{1}{\alpha \epsilon} \left| \frac{H_0^{(1)}}{H_0^{(1)'}} \right|$$

with $|H_0^{(1)'} / H_0^{(1)}| \approx 1$. Since $v = 2 \cdot 10^6$ m/s, $\epsilon = 0.07$, we have $E_c : E_s = 8 : 1$, to be compared with a ratio 16:1 estimated by KAHN and LERCHE. The geo-

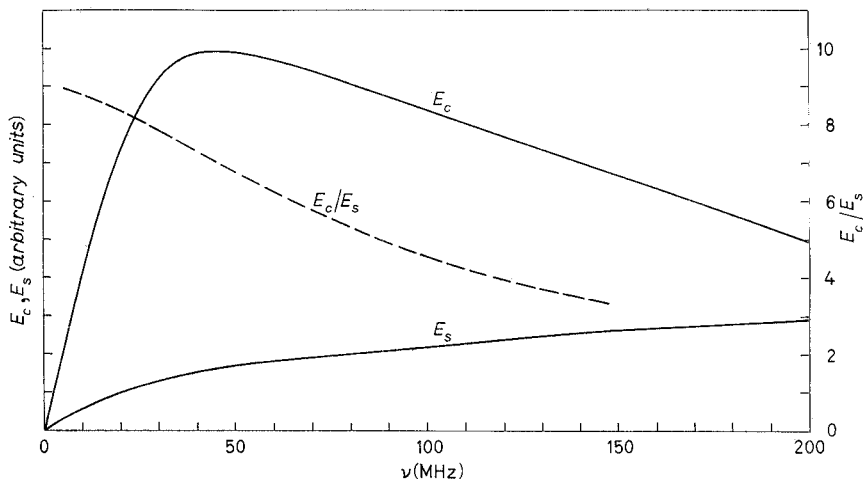


Fig. 4. — The electric field of the radiation from the transverse current E_c and space charge E_s at various frequencies, in arbitrary units (solid lines). The dashed line gives the ratio E_c/E_s .

magnetic effect prevails over the excess charge radiation, but it is less and less important the higher the frequency; the total intensity is a decreasing function of frequency above ~ 40 MHz, and the degree of polarization decreases with increasing frequency.

The dipole field turns out to be less than the current field by a large factor (~ 5 , slightly dependent on the height considered).

We assumed the disc of charges to be thin, which is reasonably correct when one deals with frequencies < 100 MHz. A Monte Carlo computation of the arrival-time distribution for the electromagnetic component of the EAS⁽²⁵⁾ has shown the shower thickness is < 2 m up to large distances from the axis. A calculation⁽²⁶⁾, by means of the diffusion equations in approximation A,

(25) M. A. LOCCI, P. PICCHI and G. VERRI: *Nuovo Cimento*, **50** A, 384 (1967).

(26) G. BOSIA and G. NAVARRA: *Nuovo Cimento*, **62** B, 301 (1969).

of the temporal distribution of electrons in EAS resulting from Coulomb scattering gives a thickness of the shower front for the mean energy of the shower electrons ~ 1.5 m, in agreement with experimental results, only slightly dependent on the shower « age » and the primary energy.

4. – Comparison with experimental data.

Coherent radio signals from EAS are now being detected at frequencies from 12 to 90 MHz (1-10). Let us discuss the experimental data, namely the dependence of the radiated power on shower size, on the distance R from the shower axis, the frequency spectrum $I(\nu)$, and the signal polarization, as to their relevance for the emission mechanism.

Measurements at Haverah Park (5) and Moscow (6) are compatible with a proportionality between pulse amplitude and primary energy E_0 , as is expected for coherent radiation, and the radial dependence has been seen (6) to be $\sim 1/R$. But the radiation from charge excess and charge separation has the same dependence on the shower size, as relations (4) and (5) show, while the radial dependence is given by $H_0^{(1)}(k\alpha R)$ and $H_0^{(1')}(k\alpha R)$, and $H_0^{(1')} \approx H_0^{(1)}$ when $k\alpha R \geq 1$.

The frequency spectrum of the radio signal has been investigated at Haverah Park (5) and Chacaltaya (7); the signal amplitude was seen to diminish with increasing frequency in the region (32–60) MHz. This agrees with our results, according to which coherence soon begins being lost at the outer rings, which give, according to (3), a large contribution to the current radiation.

The parameter suitable for experimentally investigating the relative importance of the two radiation mechanisms is the signal polarization, which has been estimated by comparing counting rates and pulse amplitudes for antennae oriented E-W from showers travelling along or across the geomagnetic field lines, and counting rates for antennae oriented E-W and N-S. A measurement performed at Jodrell Bank (8) has given no evidence for a geomagnetic effect, while the Moscow results (6) at 30.2 MHz are more consistent with a linear polarization of the signal according to Kahn and Lerche's prediction. At Calgary (9), the pulse amplitude from EAS travelling perpendicular to the Earth's magnetic field has been seen to be twice as large, on the average, as that from EAS travelling along. At Haverah Park (5) the relative numbers of radio showers, detected by antennae oriented E-W, coming from the north and south have been 73:27 at 32 MHz and 33:27 at 44 MHz. These ratios are lower than the ratio $E_c:E_s = 7.8$ and 7 at the two frequencies from our calculations. The geomagnetic field at Haverah Park is less than our value $B_\perp = 0.3$ G, and also the experimental ratios do not represent the field ratios,

because the current radiation can contribute to the signal from the antenna pointed due south, by an amount not easy to evaluate, but the results at the two frequencies, using similar method and apparatus, show that the polarization indeed decreases with increasing frequency in agreement with our predictions.

A polarization experiment has been recently performed at Chacaltaya (10) in the frequency band (50–70) MHz, with antenna systems oriented EW and NS pointing at the zenith. The geomagnetic field is nearly horizontal at Chacaltaya, and this gives good symmetry conditions. The relative counting rates at the two orientations have been 23:7, which, although statistically limited, agrees well with our ratio $E_e:E_s$ at this frequency band.

In conclusion, our analysis of the EAS development in the geomagnetic field, which takes Coulomb scattering explicitly into consideration, and gives a more accurate evaluation of the negative excess due to e^+ annihilation, shows that the geomagnetic mechanism is significant, but its importance is reduced compared with previous estimates, and decreases with increasing frequency, which seems to agree with experimental results. The best operating frequencies for detecting EAS by their radio emission seem to lie in the range (30–50) MHz, and the polarization can be best seen at the lowest frequencies.

* * *

The authors are grateful to Prof. M. AGENO, head of the Physics Laboratory at the Istituto Superiore di Sanità, for granting the use of the IBM 7040 computer.

APPENDIX

The cascade develops along the z -axis. At $t=0$ the particle is at (x_0, y_0, z_0) with velocity $\mathbf{v} = \mathbf{v}_0 = (v_{x0}, v_{y0}, v_{z0})$. In the geomagnetic field $\mathbf{B} = B\mathbf{j}$ the velocity ($v \approx c$) varies with time according to

$$(A.1) \quad \begin{cases} v_x(t) = v \cos(\omega_L t + \alpha), \\ v_y(t) = v_{y0} = \text{const}, \quad \alpha = \cos^{-1}(v_{x0}/v) = \sin^{-1}(\pm v_{z0}/v), \\ v_z(t) = \pm v_\perp \sin(\omega_L t + \alpha), \end{cases}$$

where the upper sign holds for positrons; $\omega_L = eB_\perp/\gamma mc = (8.98 \cdot 10^6 B_\perp)/E$ is the Larmor frequency (B in G, E in MeV, v in cm/s). The particle travels a distance L in the time $t \approx L/c$ between two radiation processes, its mag-

netic displacements along x , $\Delta x^{(m)} = x(t) - v_{x0}t$, is

$$(A.2) \quad \Delta x^{(m)} = \frac{c}{\omega_L} \sin \theta \cos \varphi (\omega_L t - \sin \omega_L t) \pm \cos \theta (1 - \cos \omega_L t),$$

where θ, φ are the polar angles of the velocity vector at $t=0$, the z -axis being the polar axis and φ being measured from the positive x -axis. The polar angles of the final velocity are given by

$$\begin{aligned} \cos \theta(t) &= \frac{1}{c} v_z(t), & \cos \varphi(t) &= v_x(t)/c \sin \theta(t), \\ \sin \theta(t) &= \frac{1}{c} [v_x^2(t) + v_y^2(t)]^{\frac{1}{2}}, & \sin \varphi(t) &= v_y(t)/c \sin \theta(t). \end{aligned}$$

The magnetic deviation is evaluated at an energy $E = \frac{1}{2}(E_i + E_f)$, E_i and E_f being the initial and final energy along the path L , then added to the geometrical displacement plus that contributed by Coulomb scattering to have the final position of the particle.

The mean values \bar{v}_x, \bar{v}_y are evaluated for electrons and positrons in a series of rings about the axis at the three reference heights. The current in the k -th ring is

$$\begin{aligned} J_x^{(k)} &= e(n_k^+ v_x^+ - n_k^- v_x^-), \\ J_y^{(k)} &= e(n_k^+ v_y^+ - n_k^- v_y^-), \end{aligned}$$

where n_k^+, n_k^- are the number of e^+ , e^- with $E > E_e(h)$ in the ring.

The annihilation cross-section for positrons in flight with $E \gg mc^2$ is $\sigma_{\text{ann}} \simeq \pi r_0^2 (mc^2/E) \ln(2E/mc^2)$. A beam of positrons which goes through matter is attenuated according to $N(x) = N \exp[-\tau x]$, where $\tau = \mathcal{N}(Z/A) \rho \sigma_{\text{ann}} = 3.003 \cdot 10^{23} \rho \sigma_{\text{ann}} (\text{cm}^{-1})$ in air. The computer evaluates at each path the survival probability for the positron after travelling the distance x :

$$W_{\text{no-ann}} = \exp \left[-3.829 \cdot 10^{-2} \rho \frac{\ln(3.9139 E) - 1}{E} x \right]$$

with E in MeV, ρ in g/cm³.

RIASSUNTO

Si analizza l'effetto del campo geomagnetico sull'emissione radio degli EAS simulando con un Monte Carlo tridimensionale, in cui si tiene conto dello scattering coulombiano, lo sviluppo di cascate e.m. nel campo magnetico terrestre. Il calcolo dà a varie

altezze per sciami verticali il momento di dipolo M , la corrente trasversale J e l'eccesso di carica negativa ε . Una discussione del campo di radiazione mostra che l'effetto geomagnetico è sensibilmente minore di quanto stimato in precedenza ed è funzione della frequenza. La polarizzazione del segnale osservato diminuisce al crescere della frequenza, in accordo con i dati di osservazione.

О поляризации когерентных радио-сигналов от EAS.

Резюме (*). — Анализируется влияние геомагнитного поля на радиоизлучение EAS, моделируя трехмерное развитие по Монте-Карло для е.м. каскада в магнитном поле Земли, учитывая полностью кулоновское рассеяние. Мы вычисляем для вертикальных ливней при различных высотах дипольный момент M , поперечный ток J , вместе с избытком отрицательного заряда ε . Рассмотрение радиационного поля показывает, что геомагнитный эффект значительно меньше, чем предварительные оценки, и зависит от частоты. Поляризация наблюденного сигнала заметно уменьшается с увеличением частоты, что, повидимому, согласуется с экспериментальными данными.

(*) Переведено редакцией.